



Apparent diffusion coefficient map based radiomics model in identifying the ischemic penumbra in acute ischemic stroke

Ru Zhang¹, Li Zhu¹, Zhengqi Zhu¹, Yaqiong Ge², Zhongxin Zhang³, Tianle Wang¹

¹Department of Radiology, The Second Affiliated Hospital of Nantong University, Nantong, China; ²GE Healthcare, Nanjing, China; ³Department of Ultrasound, The Second Affiliated Hospital of Nantong University, Nantong, China

Contributions: (I) Conception and design: R Zhang; (II) Administrative support: T Wang, Z Zhang; (III) Provision of study materials or patients: R Zhang, L Zhu, Z Zhu; (IV) Collection and assembly of data: R Zhang; (V) Data analysis and interpretation: R Zhang, Y Ge; (VI) Manuscript writing: All authors; (VII) Final approval of manuscript: All authors.

Correspondence to: Tianle Wang, MD, PhD. Department of Radiology, The Second Affiliated Hospital of Nantong University, Nantong 226001, China. Email: wangtianle9192@163.com; Zhongxin Zhang, MD, PhD. Department of Ultrasound, The Second Affiliated Hospital of Nantong University, Nantong 226001, China. Email: xixisi@163.com.

Background: Saving the ischemic penumbra (IP) is key in treating acute ischemic stroke (AIS). We aim to investigate the value of the apparent diffusion coefficient (ADC) map based radiomics model in the identification of IP in AIS.

Methods: This study retrospectively analyzed the data of 241 patients with AIS involving the anterior cerebral circulation who were treated in our hospital within 24 h of stroke onset from January 2014 to October 2019. With the perfusion-weighted imaging (PWI)/diffusion-weighted imaging (DWI) mismatch model as the gold standard to determine whether IP exists, we divided patients into PWI/DWI mismatch (84 cases) and non-PWI/DWI mismatch (157 cases). Following the DWI high signal area, the region of interest (ROI) was drawn to the maximum level of the lesions on the ADC map, and a total of 896 features were extracted. Maximum correlation and minimum redundancy (mRMR) algorithm were applied to select the optimized features subsets, and then the least absolute shrinkage and selection operator (LASSO) were furtherly applied to select the best features to construct radiomics signature in predicting PWI/DWI mismatch. The performance of the model was evaluated using a receiver operating characteristic (ROC) curve. One hundred times internal cross-validation was applied to evaluate the stability of the model. The clinical value of the model was evaluated using decision curve analysis (DCA).

Results: Twenty-one features were finally selected to set up the radiomics model. In the training set, the area under the ROC curve (AUC) was 0.92, and the sensitivity, specificity, and accuracy were 0.93, 0.75, 0.82, respectively. In the validation set, the AUC was 0.90, and the sensitivity, specificity, and accuracy were 0.88, 0.74, 0.80, respectively. The average AUC of internal cross-validation for 100 times in the training set were 0.88 and 0.83 in the validation set. DCA shows that within the threshold range of 0.08 to 1.0, the model gains more net benefit.

Conclusions: The radiomics model based on the ADC map can effectively determine the presence of IP in patients with AIS.

Keywords: Acute ischemic stroke (AIS); ischemic penumbra (IP); radiomics; apparent diffusion coefficient map (ADC map)

Submitted Apr 25, 2020. Accepted for publication Jul 04, 2020.

doi: 10.21037/apm-20-1142

View this article at: <http://dx.doi.org/10.21037/apm-20-1142>

Introduction

Acute ischemic stroke (AIS) is a common clinical cerebrovascular disease characterized by high morbidity, high recurrence rate, high mortality, and high disability rate. Prompt assessment of AIS patients is critical, and the treatment includes the use of recombinant tissue plasminogen activator (rt-PA), which is the cornerstone of intravascular intervention therapy (1-3). Studies have shown that patients who receive rt-PA via rapid intravenous injection within 3–4.5 h of stroke onset will have a good prognosis (4). However, not all patients can receive help from rapid intervention; thus, determining which patients would benefit is one of the significant challenges for interventional stroke management. Ischemic brain tissue can be divided into the ischemic core, the ischemic penumbra (IP), and benign oligemia (5). IP refers to the ischemic brain tissue surrounding the ischemic core that has not sustained an irreversible injury and can be recovered through prompt intervention (6). Therefore, identifying IP is a current clinical research focus.

At present, the imaging methods commonly used to identify the ischemic penumbra include: computed tomographic perfusion (CTP), magnetic resonance perfusion-weighted imaging (MR-PWI), positron emission tomography (PET) and single-photon emission computed tomography (SPECT). Both CTP and MR-PWI require contrast injection. CTP, PET and SPECT all have radiation, and PET and SPECT are not suitable for emergency examinations (7).

In the current study, an onion-like distribution of successively decreasing ADC values was found from IP toward the infarct core (8). Therefore, the ADC value can be used to predict IP.

This study aimed to investigate the value of the apparent diffusion coefficient (ADC) map based radiomics model in the identification of IP in AIS.

We present the following article in accordance with the STROBE reporting checklist (available at <http://dx.doi.org/10.21037/apm-20-1142>).

Methods

Study subjects

This study retrospectively analyzed the data of patients with AIS who were treated in our hospital from January 2014 to October 2019. The study was conducted in accordance with the Declaration of Helsinki (as revised in

2013), and was approved by the Ethics Committee of the Second Affiliated Hospital of Nantong University (No. 2020YL025). The inclusion criteria were as follows: (I) patients aged 18 years or older; (II) patients with first-onset ischemic stroke involving the anterior cerebral circulation which had undergone magnetic resonance imaging (MRI) examination within 24 h of stroke onset and had complete MRI examination data, clinical data and high-quality images (no significant motion artifacts); and (III) patients with the largest lesion size equal to or greater than 1 cm, with the lesion appearing as hyperintensity on diffusion-weighted imaging (DWI) images and decreased ADC values on ADC map. The exclusion criteria were as follows: (I) patients whose CT examination revealed cerebral hemorrhage, intracranial tumor, arteriovenous malformation, or subarachnoid hemorrhage; (II) patients with hemorrhagic transformation in AIS; and (III) patients who received thrombolysis or anticoagulation therapy before MRI.

The data of 315 patients with AIS were collected. After excluding three patients with low-quality images, two patients with incomplete clinical data, eight patients who received thrombolysis or anticoagulation therapy before MRI, 43 patients with hemorrhagic transformation in AIS, and 18 patients with the largest lesion size less than 1 cm, a total of 241 patients were eventually included in this study.

Because of the retrospective nature of the research, the requirement for informed consent was waived.

MRI equipment and methods

All patients underwent whole-brain MRI with the Siemens Verio 3.0T MRI system (Germany). The scanning sequences included conventional T1-weighted imaging (T1WI), T2-weighted imaging (T2WI), DWI, and dynamic susceptibility contrast perfusion-weighted imaging (DSC-PWI). Gadopentetate dimeglumine was used as the contrast agent for PWI and was bolus-injected into patients using high-pressure syringes at a dose of 0.1 mmol/kg and an injection rate of 4 mL/s. The scan settings for spin-echo (SE) T1WI were as follows: repetition time (TR) = 2,000 ms, echo time (TE) = 9 ms, flip angle (FA) = 150°, field of view (FOV) = 230 mm × 98.8 mm, matrix = 320 × 240, slice thickness = 5 mm, and interslice gap = 1 mm. The scan settings for SE T2WI were as follows: TR = 5,500 ms, TE = 95 s, FA = 150°, FOV = 220 mm × 100 mm, matrix = 384 × 288, slice thickness = 5 mm, and interslice gap = 1 mm. The scan settings for DWI using the SE echo-planar imaging (SE-EPI) sequence were as follows: TR

=6,600 ms, TE =100 ms, FA =90°, FOV =230 mm × 100 mm, matrix =192×192, slice thickness =5 mm, interslice gap =1 mm, and b = 0, 1,000 s/mm². The scan settings for DSC-PWI were as follows: TR =1,500 ms, TE =30 ms, FA = 90°, FOV =200 mm × 100 mm, matrix =128 × 128, slice thickness =5 mm, and interslice gap =1 mm.

Identification of IP

The collected PWI images were transferred to a postprocessing workstation, Syngo MR Workplace, where they were processed using the Perfusion software package to calculate the cerebral blood volume (CBV), cerebral blood flow (CBF), time to peak (TTP), and mean transit time (MTT) maps. Studies have shown that TTP was the most sensitive indicator of ischemia (9). So the PWI/DWI mismatch model adopted TTP/DWI mismatch. All images were measured by a radiologist with 15 years of experience in neuroimaging diagnosis. The radiologist manually delineated regions on DWI and PWI images and the volume semiautomatic measurement software for measurement. The volumes of abnormal regions on DWI and PWI were obtained using the following formula: volume = total area of abnormal regions on DWI and PWI × (thickness + interslice gap). Refer to the Endovascular Therapy Following Imaging Evaluation for Ischemic Stroke (DEFUSE 3) criteria, we determined that the PWI-DWI mismatch is a volume ratio of a region with a prolonged TTP and a region-restricted with diffusion equal to or greater than 1.8 (10).

ROI delineation

The ADC maps of all eligible patients with AIS were imported into the image processing software ITK-SNAP 3.8.0. Refer to the DWI high signal area, two radiologists with more than five years of experience in neuroimaging diagnosis (8 and 13 years) manually delineated the ROI on the slice showing the largest lesion area on each ADC map. Before delineation, the radiologists did not know whether the patients had a DWI-PWI mismatch.

Extraction of radiomics features and stability assessment

A high-throughput sampling of radiomics features from the ROI region on the ADC map of each patient with AIS was performed using GE Analysis-Kinetics analysis software (USA). The 896 extracted features included features into

seven categories: 42 histogram features, nine form factor features, 144 gray-level co-occurrence matrix (GLCM) features, 10 Haralick features, 180 run-length matrix (RLM) features, 11 gray-level size zone matrix (GLSZM) features, and 500 gradient-based features. The interclass correlation coefficient (ICC) of each feature was calculated to avoid interobserver variation during manual segmentation, and features with high stability were selected.

Construction and evaluation of the radiomics model

The patients were randomly divided into the training set (169 cases) and the validation set (72 cases) at a ratio of 7:3. At first, “maximum correlation and minimum redundancy (mRMR)” was employed to eliminate redundant and irrelevant features. Then Lasso regression analysis was conducted to choose the optimized subset of features to construct the final model. The lambda values given by the Lasso regression model were screened by 10-fold cross-validation, and the features with the nonzero coefficient were selected under the optimum lambda value for the construction of the radiomics signature. The radiomics score is the sum of the product of these features with their corresponding coefficients, as shown in the following formula: radiomics score = ($\sum \beta_i * X_i$) + intercept, where X_i and β_i are the remaining features and corresponding coefficients. The radiomics score of each patient with AIS was calculated, and then the Youden index was used to select the best radiomics score cutoff point. The patients with AIS were classified into two groups using the optimal cutoff point: patients with radiomics scores higher than the optimal cutoff point were classified into one group, and patients with radiomics scores lower than the optimal cutoff point were classified into another group. The Wilcoxon test was used to compare differences in radiomics scores between the two groups.

A receiver operating characteristic (ROC) curve was used to assess the predictive power of the radiomics score model. 100 times internal cross-validation was applied to evaluate the stability of the model. Finally, decision curve analysis (DCA) was used to assess the clinical value of the model.

Statistical analysis

SPSS 25.0 (IBM Corp.) software was used for statistical analysis of the general data in this study. Measurement data were analyzed for normality, and data conforming to a normal distribution are all expressed as the mean ± standard

Table 1 Characteristics of patients with and without PWI/DWI mismatch

Characteristics	Without PWI/DWI mismatch (n=157)	With PWI/DWI mismatch (n=84)	t/χ^2	P
Age (mean \pm SD, years)	65.20 \pm 11.47	66.17 \pm 10.69	0.636	0.526
Gender (%)			0.996	0.318
Male	109 (69.4)	53 (63.1)		
Female	48 (30.6)	31 (36.9)		
Lesion site (%)			2.481	0.115
Left	84 (53.5)	36 (42.9)		
Right	73 (46.5)	48 (57.1)		
Risk factors (%)				
Hypertension	118 (75.2)	60 (71.4)	0.394	0.530
Hyperlipemia	39 (24.8)	23 (27.4)	0.185	0.667
Hyperglycemia	53 (33.8)	34 (40.5)	1.071	0.301
Heart diseases such as atrial fibrillation and valvulopathy	30 (19.1)	13 (15.5)	0.492	0.483
Smoking	85 (54.1)	42 (50.0)	0.376	0.540

PWI, perfusion-weighted imaging; DWI, diffusion-weighted imaging.

deviation ($\bar{x} \pm S$). Differences between the two groups were compared using an independent-sample t -test. Categorical and count data are expressed as the number of cases (percentage), and differences between two groups were compared using the χ^2 test. P values less than 0.05 were considered statistically significant.

The ICC was used to evaluate the interobserver reliability of the radiomics features extracted by the two radiologists. Features with an ICC ≥ 0.8 were selected.

R language (Version 3.5.1, WWW.R-project.org) was used for the statistical analysis. First, the “mRMR” package was used to cut redundant and irrelevant features. Lasso regression was conducted using the “glmnet” package to construct the radiomics model. ROC curves were evaluated using the “pROC” package to assess the prediction ability of the radiomics score model. DCA was performed using the “rmda” package to assess the clinical value of the model.

Results

General data of the patients

The data were analyzed according to the inclusion and exclusion criteria. A total of 241 patients were eventually included, including 162 male patients and 79 female patients aged 35–93 years, with an average age of 65.5 \pm 11.2 years.

The statistical results for general clinical data are shown below (Table 1).

The two groups of patients showed no significant differences in general clinical data, including age, gender, lesion site, hypertension, hyperlipidemia, hyperglycemia, and heart diseases such as atrial fibrillation and valvulopathy ($P > 0.05$).

Interobserver reliability for radiomics feature extraction

The ICC values of the 896 radiomics features extracted by the two radiologists were in the range of (2.0903e-16–0.99960). This study selected 728 features with an ICC ≥ 0.80 , which showed high stability and interobserver reliability.

Construction of the radiomics model

Firstly, the mRMR method was adopted to screen the 728 features with high stability in the training set. After cutting redundant and irrelevant features, 30 features were kept. Then, the Lasso regression analysis was conducted to choose the optimized subset of features to construct the final model (Figure 1A,B). The lambda values given by the Lasso regression model were screened by 10-fold cross-

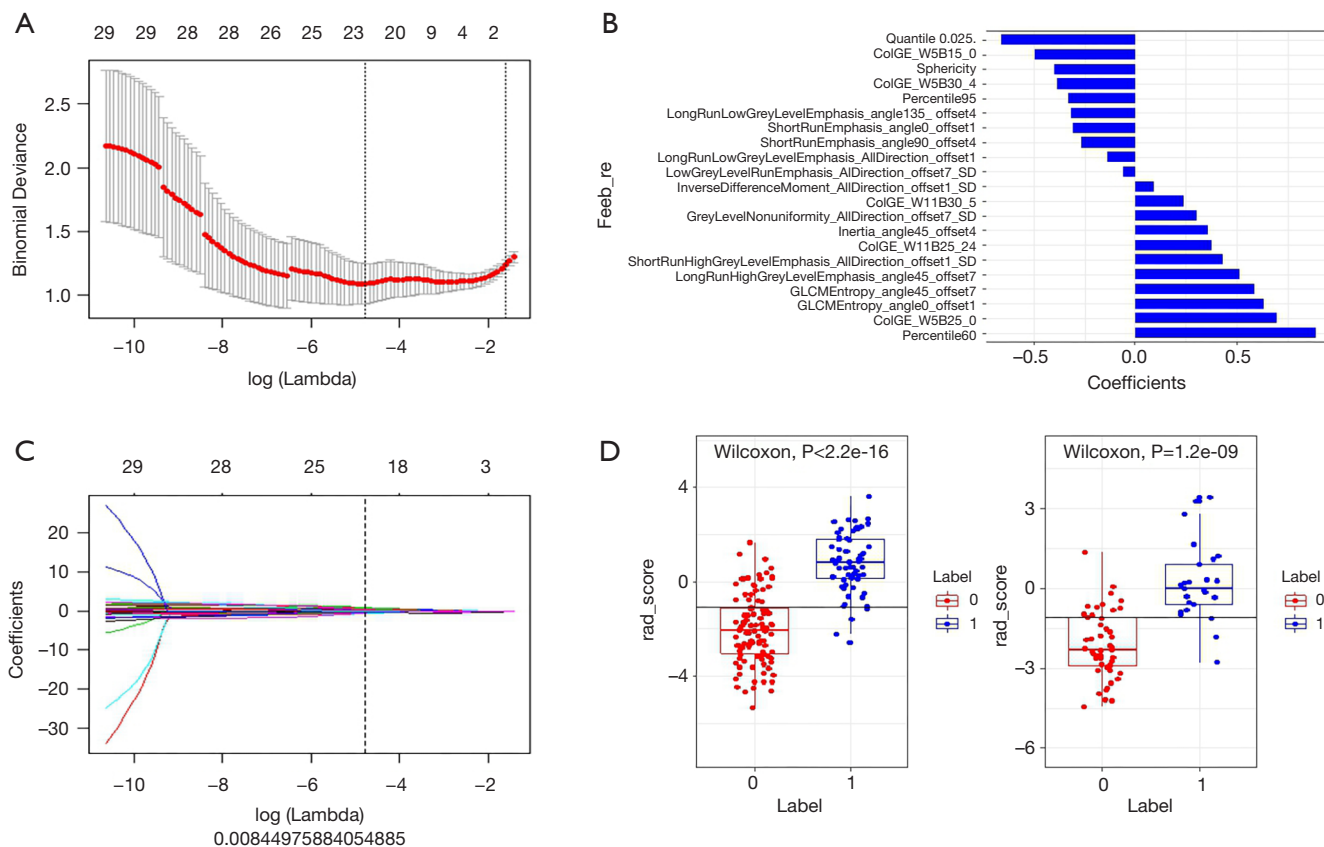


Figure 1 LASSO feature selection and model construction. (A) The 10-fold cross-validation of the LASSO analysis was performed to pick up the optimal lambda value. (B) The regression coefficients of LASSO. (C) Twenty-one features with nonzero coefficients were kept, and their corresponding coefficients were shown. (D) The boxplot shows the Rad score to classify the patients into PWI/DWI mismatch group or without a PWI/DWI mismatch group based on cutoff value. Below the cutoff value, without PWI/DWI mismatch [0], and above the cutoff value, with PWI/DWI mismatch [1]. Wilcoxon test showed there was a significant difference between patients with and without PWI/DWI mismatch. LASSO, least absolute shrinkage and selection operator; PWI, perfusion-weighted imaging; DWI, diffusion-weighted imaging.

validation, and the features with a nonzero coefficient were selected under the optimum lambda value for the construction of the radiomics score model (Figure 1C). The final retained features are shown in Table 2.

Using the formulas radiomics score = ($\sum \beta_i * X_i$) + intercept, the Radiomics score = $-0.397 * \text{Sphericity} + 0.317 * \text{LongRunLowGreyLevelEmphasis_angle135_offset4} + 0.891 * \text{Percentile60} + 0.375 * \text{ColGE_W11B25_24} + -0.265 * \text{ShortRunEmphasis_angle90_offset4} + -0.136 * \text{LongRunLowGreyLevelEmphasis_AllDirection_offset1} + 0.7 * \text{ColGE_W5B25_0} + 0.635 * \text{GLCMEntropy_angle0_offset1} + 0.431 * \text{ShortRunHighGreyLevelEmphasis_AllDirection_offset1_SD} + 0.303 * \text{GreyLevelNonuniformity_AllDirection_offset7_SD} + -0.058 * \text{LowGreyLevelRunEm}$

$\text{phasis_AllDirection_offset7_SD} + 0.512 * \text{LongRunHighGreyLevelEmphasis_angle45_offset7} + 0.238 * \text{ColGE_W11B30_5} + 0.092 * \text{InverseDifferenceMoment_AllDirection_offset1_SD} + -0.329 * \text{Percentile95} + -0.657 * \text{Quantile0.025} + -0.495 * \text{ColGE_W5B15_0} + -0.385 * \text{ColGE_W5B30_4} + 0.588 * \text{GLCMEntropy_angle45_offset7} + -0.306 * \text{ShortRunEmphasis_angle0_offset1} + 0.36 * \text{Inertia_angle45_offset4} + -1.029$, the radiomics scores of each AIS patient were calculated. Then, the best cutoff point of -0.106 was selected for the radiomics score using the Youden index. The Wilcoxon test was used to compare the differences between the two groups of patients with AIS. The P values in both the training and test datasets were <0.05 , and the differences were statistically significant

Table 2 The final retained features

Features	Coefficient	Odds ratio	Lower	Upper	P value
Sphericity	-0.397	0.276499	0.180115	0.424462	4.14E-09
LongRunLowGreyLevelEmphasis_angle135_offset4	-0.317	5.03E-10	6.52E-31	3.88E+11	0.382926
Percentile60	0.891	1.516905	1.095493	2.100425	0.012101
ColGE_W11B25_24	0.375	3.077529	1.969222	4.809609	8.03E-07
ShortRunEmphasis_angle90_offset4	-0.265	0.75286	0.55025	1.030073	0.075943
LongRunLowGreyLevelEmphasis_AllDirection_offset1	-0.136	0.937111	0.650181	1.350667	0.727648
ColGE_W5B25_0	0.700	2.757326	1.823631	4.169071	1.52E-06
GLCMEntropy_angle0_offset1	0.635	2.607514	1.66074	4.094038	3.13E-05
ShortRunHighGreyLevelEmphasis_AllDirection_offset1_SD	0.431	1.280589	0.717637	2.285149	0.40257
GreyLevelNonuniformity_AllDirection_offset7_SD	0.303	2.350464	0.86919	6.356123	0.092229
LowGreyLevelRunEmphasis_AllDirection_offset7_SD	0.058	0.591322	0.1425	2.336546	0.006775
LongRunHighGreyLevelEmphasis_angle45_offset7	0.512	1.127621	0.825553	1.540214	0.450263
ColGE_W11B30_5	0.238	2.762145	1.862053	4.09733	4.42E-07
InverseDifferenceMoment_AllDirection_offset1_SD	0.092	1.307296	0.95356	1.792255	0.096
Percentile95	-0.329	1.406807	1.023453	1.933753	0.035485
Quantile0.025	-0.657	0.832468	0.604016	1.147325	0.262593
ColGE_W5B15_0	-0.495	2.415192	1.573645	3.706777	5.48E-05
ColGE_W5B30_4	-0.385	1.473504	1.01524	2.138621	0.041396
GLCMEntropy_angle45_offset7	0.588	4.138863	2.187905	7.829493	1.26E-05
ShortRunEmphasis_angle0_offset1	-0.306	0.886804	0.652783	1.204721	0.442188
Inertia_angle45_offset4	0.360	0.682659	0.468415	0.994894	0.046967
Rad score	-1.029	4.009493	2.647332	6.072542	5.50E-11

(Figure 1D).

Evaluation of the diagnostic efficacy of the radiomics score model

The ROC curves were used to evaluate the diagnostic efficacy of the radiomics score model (Figure 2A,B). The area under the ROC curve (AUC) of the training set was 0.92 [95% confidence interval (CI): 0.88–0.96], and the sensitivity, specificity, positive predictive value (PPV), negative predictive value (NPV), and accuracy of the training set were 0.93, 0.75, 0.67, 0.95 and 0.82, respectively. The AUC of the validation set was 0.90 (95% CI: 0.82–0.98), and the sensitivity, specificity, PPV, NPV, and accuracy of the test dataset were 0.88, 0.74, 0.65, 0.92 and 0.80, respectively.

Internal cross-validation

Internal cross-validation was performed by resampling different patients into training and validation groups for 100 times and get the average AUC value were calculated to assess the stability of the model (Figure 2C), the mean value of the 100 AUCs and std were 0.88 and 0.03 in the training set and 0.83, 0.05 in the validation set, which means high reliability of the model.

Decision curve analysis

The DCA can help determine the clinical application value of the radiomics score model. DCA showed that within a threshold range of 0.08–1.0, the net benefit of the model is large and that the model can be relatively safely used to

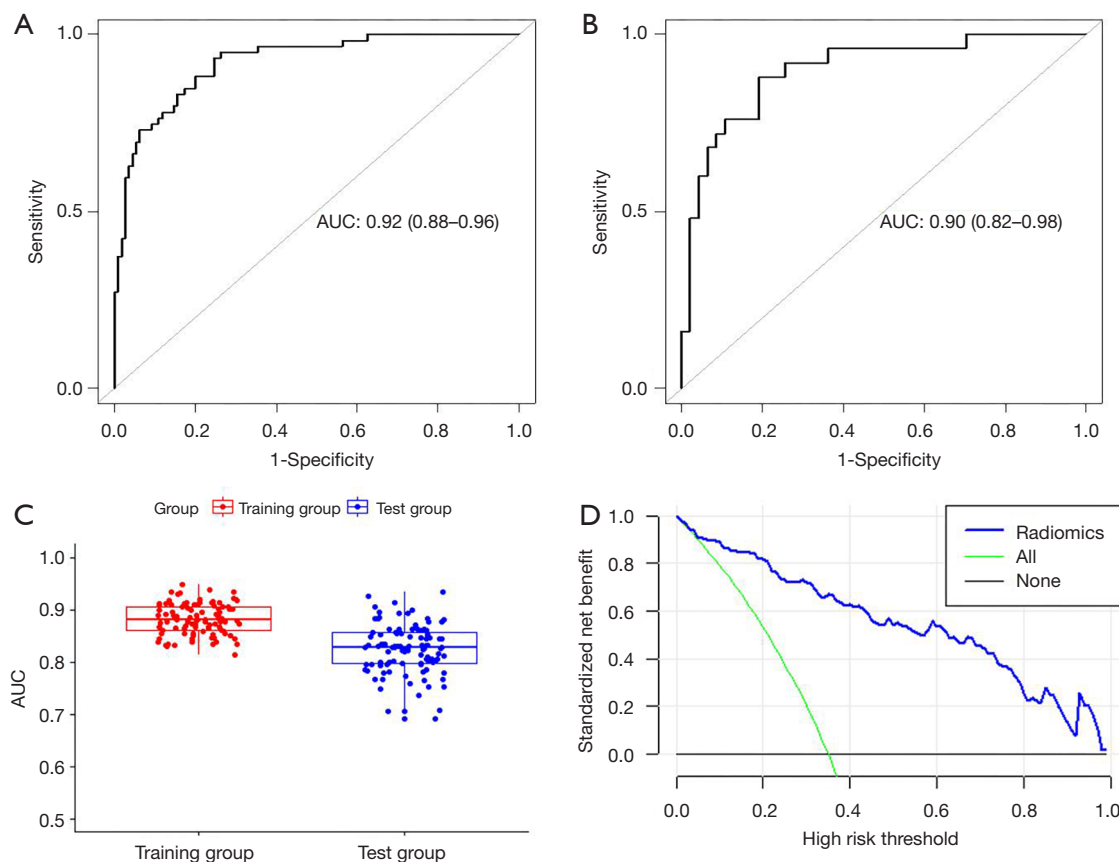


Figure 2 Validation of the model and its clinical use. (A) ROC curve of the training set. (B) ROC curve of the validation set. (C) The boxplot shows the results of internal validation by resampling different patients into training and validation groups for 100 times. (D) The decision curve analyzes for the radiomics signature. The y-axis is the net benefit. The black curve means that no patients with PWI/DWI mismatch, the green curve means all patients had PWI/DWI mismatch, while the blue curve represents that during the threshold of 0.08 to 1, the radiomics model gains more net benefit than other two cases. ROC, receiver operating characteristic; PWI, perfusion-weighted imaging; DWI, diffusion-weighted imaging.

predict the presence of PWI-DWI mismatch in patients with AIS (Figure 2D).

Discussion

Currently, the most used method for IP identification is the PWI-DWI mismatch model (11). PWI has drawbacks such as the need for contrast agent injection, nonuniform parameters, complicated execution, and delayed MRI examination; therefore, its application in clinical practice is limited.

In recent years, studies have shown that regions with decreased ADC values in patients with AIS include not only the infarct core but also the IP, which can be recovered

(12,13). A study on rats showed that ADC values could be used to assess the degree of blood supply to brain tissue to determine whether the tissue can be recovered (14). Nagesh *et al.* analyzed the data of nine patients with AIS within ten h of stroke onset and proposed that the ADC value can potentially identify the IP in patients with acute cerebral infarction (15).

Radiomics refers to a method that uses computer software to extract a large number of quantitative features from radiographic medical images followed by machine learning methods and/or statistical methods to select the most valuable features to improve diagnostic accuracy and predictions (16). Compared with conventional assessments of radiographic images that rely on the subjective judgment

and experience of radiologists, radiomics supplies objective information about lesions that cannot be directly observed from radiographic images. Therefore, radiomics has potential clinical value. In this study, we used the mRMR and Lasso to select 21 features from ADC maps to construct the radiomics score model. This model showed high value for identifying IP in patients with AIS. In the training set, the AUC was 0.92, and the sensitivity, specificity, PPV, NPV, and accuracy were 0.93, 0.75, 0.67, 0.95, and 0.82, respectively. In the validation set, the AUC was 0.90, and the sensitivity, specificity, PPV, NPV, and accuracy were 0.88, 0.74, 0.65, 0.92, and 0.80, respectively. The ICC between each feature was calculated to avoid interobserver variations in the manual delineation of ROIs, and the features with an ICC ≥ 0.80 were selected to ensure the stability of the features extracted after manual delineation of ROIs.

The limitations of the present study are as follows: (I) this study was a single-center retrospective study and lacked multicenter validation. (II) In this study, features were extracted only from the slice showing the largest lesion area in each patient with AIS, the features may not adequately reflect the overall situation of regions with reduced ADCs. (III) In this study, due to limitations of the postprocessing software, TTP maps were used to identify ischemic areas on PWI, and the maps of the time to peak of the residue function (Tmax) with a strict threshold were not selected. Further studies are needed.

In summary, the radiomics model based on the ADC map, can effectively determine the presence of IP in patients with AIS. The model is a simple and practical method that can be applied in clinical practice.

Acknowledgments

Funding: Supported by the grant of Science Foundation of Nantong (MS12018087, MS12018042) and the grant of Science Foundation of Jiangsu Commission of Health (H2019057).

Footnote

Reporting Checklist: The authors have completed the STROBE reporting checklist. Available at <http://dx.doi.org/10.21037/apm-20-1142>

Data Sharing Statement: Available at <http://dx.doi.org/10.21037/apm-20-1142>

Conflicts of Interest: All authors have completed the ICMJE uniform disclosure form (available at <http://dx.doi.org/10.21037/apm-20-1142>). The authors report grants from the grant of Science Foundation of Nantong, grants from the grant of Science Foundation of Jiangsu Commission of Health, during the conduct of the study

Ethical Statement: The authors are accountable for all aspects of the work in ensuring that questions related to the accuracy or integrity of any part of the work are appropriately investigated and resolved. The study was conducted in accordance with the Declaration of Helsinki (as revised in 2013), and was approved by the Ethics Committee of the Second Affiliated Hospital of Nantong University (No. 2020YL025). Because of the retrospective nature of the research, the requirement for informed consent was waived.

Open Access Statement: This is an Open Access article distributed in accordance with the Creative Commons Attribution-NonCommercial-NoDerivs 4.0 International License (CC BY-NC-ND 4.0), which permits the non-commercial replication and distribution of the article with the strict proviso that no changes or edits are made and the original work is properly cited (including links to both the formal publication through the relevant DOI and the license). See: <https://creativecommons.org/licenses/by-nc-nd/4.0/>.

References

1. Fransen PS, Berkhemer OA, Lingsma HF, et al. Time to reperfusion and treatment effect for acute ischemic stroke: a randomized clinical trial. *JAMA Neurol* 2016;73:190-6.
2. Campbell BC, Mitchell PJ, Yan B, et al. A multicenter, randomized, controlled study to investigate EXtending the time for Thrombolysis in Emergency Neurological Deficits with Intra-Arterial therapy (EXTEND-IA). *Int J Stroke* 2014;9:126-32.
3. Gu HQ, Yang X, Rao ZZ, et al. Disparities in outcomes associated with rural-urban insurance status in China among inpatient women with stroke: a registry-based cohort study. *Ann Transl Med* 2019;7:426.
4. Del Zoppo GJ, Saver JL, Jauch EC, et al. Expansion of the time window for treatment of acute ischemic stroke with intravenous tissue plasminogen activator: a science advisory from the American Heart Association/American Stroke Association. *Stroke* 2009;40:2945-8.
5. Davis S, Donnan GA. Time is penumbra: imaging,

- selection and outcome. The Johann jacob wepfer award 2014. *Cerebrovasc Dis* 2014;38:59-72.
6. Hirano T. Searching for salvageable brain: the detection of ischemic penumbra using various imaging modalities? *J Stroke Cerebrovasc Dis* 2014;23:795-8.
 7. Wey HY, Desal VR, Duong TQ. A review of current imaging methods used in stroke research. *Neurol Res* 2013;35:1092-102.
 8. Fiehler J, Knab R, Reichenbach JR, et al. Apparent diffusion coefficient decreases and magnetic resonance imaging perfusion parameters are associated in ischemic tissue of acute stroke patients. *J Cereb Blood Flow Metab* 2001;21:577-84.
 9. Kamath A, Smith WS, Powers WJ, et al. Perfusion CT compared to H₂(15)O/O(15)O PET in patients with chronic cervical carotid artery occlusion. *Neuroradiology* 2008;50:745-51.
 10. Albers GW, Marks MP, Kemp S, et al. Thrombectomy for stroke at 6 to 16 hours with selection by perfusion imaging. *N Engl J Med* 2018;378:708-18.
 11. Chen F, Ni YC. Magnetic resonance diffusion-perfusion mismatch in acute ischemic stroke: An update. *World J Radiol* 2012;4:63-74.
 12. Nicoli F, Lefur Y, Denis B, et al. Metabolic counterpart of decreased apparent diffusion coefficient during hyperacute ischemic stroke: a brain proton magnetic resonance spectroscopic imaging study. *Stroke* 2003;34:e82-7.
 13. Guadagno JV, Warburton EA, Jones PS, et al. How affected is oxygen metabolism in DWI lesions?: a combined acute stroke PET-MR study. *Neurology* 2006;67:824-9.
 14. Lo EH, Pierce BA, Mandeville JB, et al. Neuroprotection with NBQX in rat focal cerebral ischemia. Effects on ADC probability distribution functions and diffusion-perfusion relationships. *Stroke* 1997;28:439-46; discussion 446-7.
 15. Nagesh V, Wjlc KM, Windham JP, et al. Time course of ADCw changes in ischemic stroke: beyond the human eye! *Stroke* 1998;29:1778-2.
 16. Lambin P, Rios-Velazquez E, Leijenaar R, et al. Radiomics: extracting more information from medical images using advanced feature analysis. *Eur J Cancer* 2012;48:441-6.
- (English Language Editor: J. Chapnick)

Cite this article as: Zhang R, Zhu L, Zhu Z, Ge Y, Zhang Z, Wang T. Apparent diffusion coefficient map based radiomics model in identifying the ischemic penumbra in acute ischemic stroke. *Ann Palliat Med* 2020;9(5):2684-2692. doi: 10.21037/apm-20-1142